

**Immunologic characterization of COVID-19 patients with hematological cancer**

Catarina Maia,<sup>1,2,3,4\*</sup> Esperanza Martín-Sánchez,<sup>1,2,3,4\*</sup> Juan José Garcés,<sup>1,2,3,4\*</sup> Ascensión López-Díaz de Cerio,<sup>1,3,5\*</sup> Susana Inogés,<sup>1,3,5</sup> Manuel F. Landeche,<sup>1</sup> Belén Gil-Alzugaray,<sup>6</sup> Cristina Perez,<sup>2,3,4</sup> Cirino Botta,<sup>7</sup> Aintzane Zabaleta,<sup>1,2,3,4</sup> Félix Alegre,<sup>1</sup> César Rincón,<sup>6</sup> Laura Blanco,<sup>3,4</sup> Sarai Sarvide,<sup>2,3,4</sup> Amaia Vilas-Zornoza,<sup>2,3,5</sup> Diego Alignedani,<sup>1,2,3,4</sup> Cristina Moreno,<sup>1,3,4</sup> Artur Paiva,<sup>8</sup> António Martinho,<sup>9</sup> Rui Alves,<sup>8</sup> Enrique Colado,<sup>10</sup> Covadonga Quirós,<sup>10</sup> Mónica Olid,<sup>6</sup> Andrés Blanco,<sup>1</sup> Josepmaria Argemi,<sup>1,3</sup> Bruno Paiva<sup>1,2,3,4#</sup> and José Ramón Yuste<sup>1,3#</sup>

<sup>1</sup>Clinica Universidad de Navarra, Pamplona, Spain; <sup>2</sup>Centro de Investigación Médica Aplicada (CIMA), Pamplona, Spain; <sup>3</sup>Instituto de Investigación Sanitaria de Navarra (IdiSNA), Pamplona, Spain; <sup>4</sup>CIBER-ONC (CB16/12/00369), Pamplona, Spain; <sup>5</sup>CIBER-ONC (CB16/12/00489), Pamplona, Spain; <sup>6</sup>Clinica Universidad de Navarra, Madrid, Spain; <sup>7</sup>Hospital "Annunziata", Cosenza, Italy; <sup>8</sup>Centro Hospitalar e Universitário de Coimbra, Coimbra, Portugal; <sup>9</sup>Centro de Sangue e Transplantação de Coimbra, Instituto Português do Sangue e da Transplantação, Coimbra, Portugal and <sup>10</sup>Hospital Universitario Central de Asturias, Oviedo, Spain

\*CM, EM-S, JJG and AL-DC contributed equally as co-first authors.

#BP and JRY contributed equally as co-senior authors.

Correspondence: JOSE' RAMON YUSTE - jryuste@unav.es

doi:10.3324/haematol.2020.269878

**Immunologic characterization of COVID-19 patients with hematological cancer**

**Authors:** Catarina Maia<sup>1,2,3,4\*</sup>, Esperanza Martín-Sánchez<sup>1,2,3,4\*</sup>, Juan José Garcés<sup>1,2,3,4\*</sup>, Ascensión López-Díaz de Cerio<sup>1,3,5\*</sup>, Susana Inogés<sup>1,3,5</sup>, Manuel F. Landecho<sup>1</sup>, Belén Gil-Alzugaray<sup>6</sup>, Cristina Perez<sup>2,3,4</sup>, Cirino Botta<sup>7</sup>, Aintzane Zabaleta<sup>1,2,3,4</sup>, Félix Alegre<sup>1</sup>, César Rincón<sup>6</sup>, Laura Blanco<sup>3,4</sup>, Sarai Sarvide<sup>2,3,4</sup>, Amaia Vilas-Zornoza<sup>2,3,5</sup>, Diego Alignani<sup>1,2,3,4</sup>, Cristina Moreno<sup>1,3,4</sup>, Artur Paiva<sup>8</sup>, António Martinho<sup>9</sup>, Rui Alves<sup>8</sup>, Enrique Colado<sup>10</sup>, Covadonga Quirós<sup>10</sup>, Mónica Olid<sup>6</sup>, Andrés Blanco<sup>1</sup>, Josepmaria Argemi<sup>1,3</sup>, Bruno Paiva<sup>1,2,3,4\*\*</sup> and José Ramón Yuste<sup>1,3\*\*</sup>

\*Co-first authors; contributed equally to this manuscript

\*\*Co-senior authors; contributed equally to this manuscript

**Affiliations:** 1) Clínica Universidad de Navarra, Pamplona, Spain; 2) Centro de Investigación Médica Aplicada (CIMA), Pamplona, Spain; 3) Instituto de Investigación Sanitaria de Navarra (IdiSNA), Pamplona, Spain; 4) CIBER-ONC number CB16/12/00369, Pamplona, Spain; 5) CIBER-ONC number CB16/12/00489, Pamplona, Spain; 6) Clínica Universidad de Navarra, Madrid, Spain; 7) Hospital “Annunziata”, Cosenza, Italy; 8) Centro Hospitalar e Universitário de Coimbra, Coimbra, Portugal; 9) Centro de Sangue e Transplantação de Coimbra, Instituto Português do Sangue e da Transplantação, Coimbra, Portugal; 10) Hospital Universitario Central de Asturias, Oviedo, Spain.

**Address for correspondence:**

José Ramón Yuste, MD, PhD

Clínica Universidad de Navarra, Pamplona, Spain

Av. Pío XII 36, 31008 Pamplona, Spain

e-mail: [jryuste@unav.es](mailto:jryuste@unav.es)

**TABLE OF CONTENT**

Supplemental Methods.....	3
References.....	5
Supplemental Table 1.....	6
Supplemental Figure 1.....	7
Supplemental Figure 2.....	8
Supplemental Figure 3.....	9

## SUPPLEMENTAL METHODS

**Multidimensional flow cytometry (MFC).** EDTA anti-coagulated peripheral blood (PB) samples were stained with the 8-color combination of the monoclonal antibodies (mAb) CD3-V450, CD45-OC515, CD20-FITC, CD16-PE, CD4-PerCPCy5.5, CD19-PECy7, CD56-APC, CD8-APCH7, lysed for 30 min and measured directly without centrifugation and washing steps to minimize risk of infection in a FACSCanto II flow cytometer (Beckton Dickinson –BD– Biosciences, San Jose, CA, USA) using the FACSDiva 6.1 software (BD, San Jose, CA, USA). Data was analyzed using automated clustering (described below). In a subset of COVID-19 patients (N = 14), PB B and T cells were characterized using EuroFlow panels for primary immunodeficiencies <sup>1</sup>, and samples were processed with the EuroFlow lyse-wash-and-stain standard sample preparation protocol (SOP) adjusted to 10<sup>5</sup> nucleated cells. Data was acquired in a FACSLyric flow cytometer (BD Biosciences, San Jose, CA) using the FACSSuite v1.3.0.6137 software (BD), and analyzed with the Infinicyt software (Cytognos SL, Salamanca, Spain).

**Automated clustering.** We used *FlowSOM* (version 1.14.1) <sup>2</sup> for automated clustering. Briefly, it is based on a four-step approach: 1) reading data; 2) building a self-organizing map (SOM) for clustering and dimensionality reduction; 3) building a minimum spanning tree to connect nodes according to their similarity; and 4) computing an automated meta-clustering by grouping similar nodes. The meta-clustering step is critical for the definition of cell populations. In this phase, groups of similar nodes are “fused” to obtain more consistent populations following specific algorithms. We used the *ConsensusClusterPlus* <sup>3</sup> (version 1.46.0) package separated from *FlowSOM* to obtain better control of each function. Clonal B cells clustering according to their bright CD19 expression and dim reactivity for CD20 were excluded from the whole B-cell cluster in patients with B-cell lymphoproliferative disorders. However, it should be noted that the combination of monoclonal antibodies described above and the number of cells measured per sample, are not empowered to detect small B-cell clones in subjects with unknown history of monoclonal B-cell lymphocytosis.

**Fluorescence-activated cell sorting (FACS).** Various myeloid subsets and antigen-presenting cells were stained using the mAb combination – HLADR-PacB, CD45-OC515, CD15-FITC, CD203c-PE, CD33-PerCPCy5.5, CD16-PECy7, CD123-APC, CD14-APCH7 – and isolated in a MoFlo Astrios EQ sorter (Beckman Coulter, CA,

USA). Based on its six-way sorting, basophils, myeloid and plasmacytoid dendritic cells, classical and non-classical monocytes and neutrophils were simultaneously isolated from PB samples of 13 COVID-19 patients. All cell types were successfully isolated in all cases except for plasmacytoid dendritic cells and basophils in 2 patients. Cells were stored in Lysis/Binding Buffer (Invitrogen™, CA, USA).

**RNA sequencing (RNAseq) and data analysis.** RNAseq was performed using a protocol adapted from massively parallel single-cell RNA-sequencing<sup>4</sup>, which enabled preparing libraries with as few cells as starting material. Briefly, we barcoded RNA from each sample in a retrotranscription (RT) reaction with AffinityScript Multiple Temperature Reverse Transcriptase (Agilent, Santa Clara, CA, USA) and different RT primers. After qPCR, cDNA with similar Ct values were pooled together. cDNA was purified with SPRIselect 1.2X (Beckman Coulter –BC–, Brea, CA, USA) and amplified using the T7 polymerase (New England Biolabs – NEB–, Ipswich, MA, USA) and the T7 promoter as template, previously introduced in the RT reaction. Samples were incubated for 16 hours at 37°C. RNA molecules were fragmented with 2 µL of 10X Zn<sup>2+</sup> fragmentation buffer (Ambion™, ThermoFisher, Waltham, MA, USA) for 1 min at 70°C and purified with SPRIselect 2X. Afterwards, a ssRNA adaptor (Illumina, San Diego, CA, USA) was ligated to the 3'-end of the RNA fragments in presence of DMSO, 100 mM ATP, 50% PEG and T4 RNA ligase I (NEB, Ipswich, MA, USA) for 2 hours at 22°C. A second RT reaction was performed with AffinityScript Multiple Temperature Reverse Transcriptase and resulting cDNA was purified with SPRIselect 1.5X. Finally, cDNA was amplified with 12.5 µL Kappa Hifi ready mix + 1µL of primer mix at 25 µM per sample and purified with SPRIselect 0.7X. Qubit, TapeStation and qPCR analyses were done as quality controls and the final library products at 4 nM were sequenced in a NextSeq (Illumina, San Diego, CA, USA).

Differential gene expression across all pairwise comparisons (hematological vs no cancer) of sorted immune populations was analyzed with *Deseq2* R package (version 1.28.1).<sup>5</sup> Data is available in the GEO database with the accession number GSE153610.

**Statistical analysis.** The Kruskal-Wallis and Mann Whitney tests were used to estimate the statistical significance observed between groups. Statistical analyses were performed using the GraphPad Prism software (version 7, San Diego, CA, USA), SPSS (version 25.0.0, IBM, Chicago, IL, USA) and R (versions 3.5.1 and 4.0.0 for MFC and RNAseq studies, respectively). *P* values < .05 were considered as statistically significant.

## REFERENCES

1. van Dongen JJM, van der Burg M, Kalina T, et al. EuroFlow-Based Flowcytometric Diagnostic Screening and Classification of Primary Immunodeficiencies of the Lymphoid System. *Front Immunol* 2019;10:1271.
2. Van Gassen S, Callebaut B, Van Helden MJ, et al. FlowSOM: Using self-organizing maps for visualization and interpretation of cytometry data. *Cytometry A* 2015;87(7):636–645.
3. Wilkerson MD, Hayes DN. ConsensusClusterPlus: a class discovery tool with confidence assessments and item tracking. *Bioinformatics* 2010;26(12):1572–1573.
4. Jaitin DA, Kenigsberg E, Keren-Shaul H, et al. Massively parallel single-cell RNA-seq for marker-free decomposition of tissues into cell types. *Science* 2014;343(6172):776–779.
5. Love MI, Huber W, Anders S. Moderated estimation of fold change and dispersion for RNA-seq data with DESeq2. *Genome Biol* 2014;15(12):550.

**Supplemental Table 1.** Demographics and clinical course of patients with COVID-19 and hematological cancer (N = 10).

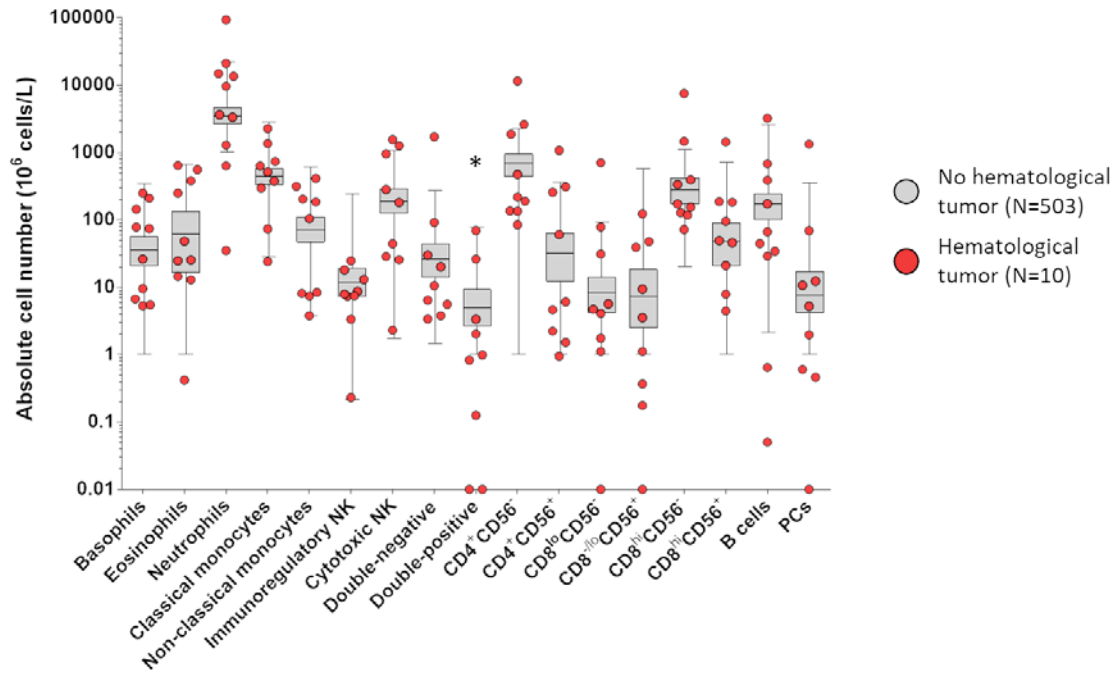
<b>Patient - Disease</b>	<b>Sex</b>	<b>Age</b>	<b>Clinical course until immune monitoring</b>	<b>Time between anticancer treatment and COVID-19</b>
1 - IgM MGUS	M	74	Asymptomatic	NA
2 - CLL	M	77	Early stage, untreated	NA
3 - IgG MGUS	M	88	Asymptomatic	NA
4 - CLL	M	62	Early stage, untreated	NA
5 - CLL	M	57	Early stage, untreated	NA
6 - AML	F	64	Secondary to MDS that was secondary to NHL. Studied in CR after allogenic stem cell transplantation	1 month
7 - DLBCL	F	31	Studied in CR after 6 cycles with R-CVP	12 months
8 - Follicular lymphoma	F	71	Studied after 1 cycle of R-CVP	On treatment
9 - MBL	M	89	Asymptomatic	NA
10 - MDS	M	86	Newly-diagnosed	NA

MGUS, monoclonal gammopathy of undetermined significance; CLL, chronic lymphocytic leukemia; AML, acute myeloid leukemia; MDS, myelodysplastic syndrome; NA: not applicable; NHL: non-Hodgkin lymphoma; CR, complete remission; DLBCL, diffuse large B-cell lymphoma; R-CVP, rituximab, cyclophosphamide, vincristine and prednisone; MBL, monoclonal B-cell lymphocytosis

**Supplemental Figure 1. Absolute number of immune cell types in COVID-19 patients with (N = 10) and without (N = 503) blood cancer.**

PCs: plasma cells

\*, P < .05

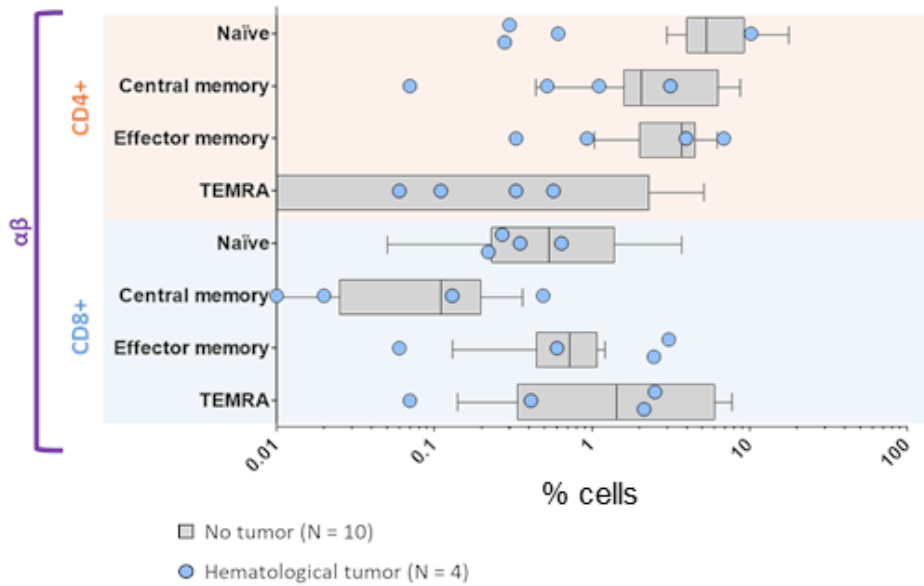


**Supplemental Figure 2. Antigen-specific differentiation of adaptive immune cells after SARS-CoV-2 infection.** Relative distribution of various **(A)** T and **(B)** B cell subsets in COVID-19 patients without cancer (N = 10) and those with hematological malignancies (N = 4).

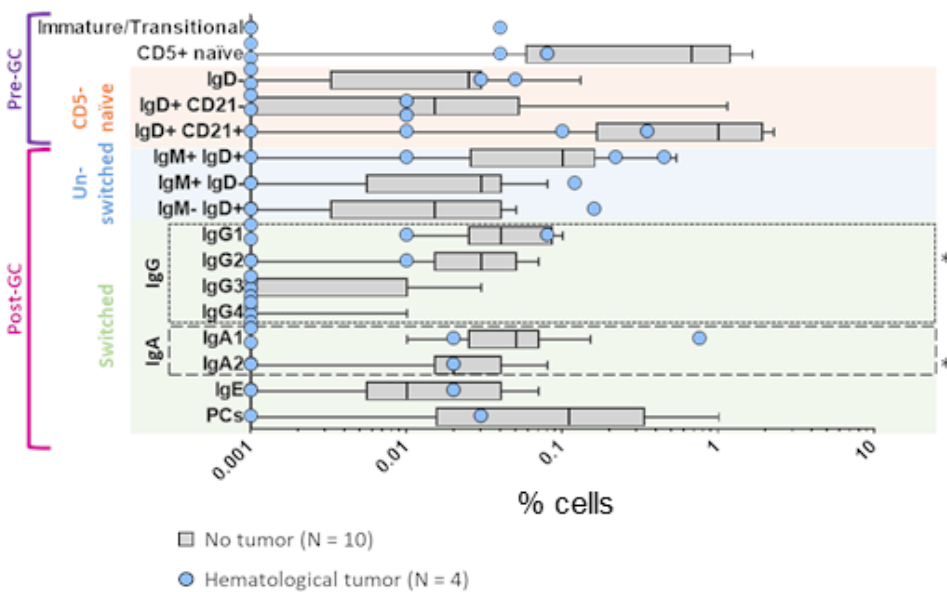
TEMRA: T cell effector memory CD45RA+; GC: germinal center; PCs: plasma cells

\*,  $P < .05$

**A**



**B**



**Supplemental Figure 3. Transcriptional status of myeloid and antigen-presenting cells in patients with COVID-19 and hematological cancer. (A)** Unsupervised correlation (Pearson's method) heatmap based on RNAseq data from basophils, myeloid and plasmacytoid dendritic cells, classical and non-classical monocytes as well as neutrophils from COVID-19 patients with (N = 3) or without (N = 10) hematological cancer. **(B)** Volcano plots based on gene expression of basophils, myeloid and plasmacytoid dendritic cells, classical and non-classical monocytes as well as neutrophils from COVID-19 patients with (N = 3) or without (N = 10) hematological cancer. Each dot corresponds to an individual gene. Differentially expressed genes (minimum  $\log_2$  fold-change and adjusted  $P$  value < .05) were given a unique color for each cell type: basophils (dark yellow, n=112 infra/19 overexpressed), myeloid (green, n=9/1) and plasmacytoid (dark blue, n=495/43) dendritic cells, classical (cyan, n=188/56) and non-classical (grey, n=26/13) monocytes as well as neutrophils (red, n=436/81). Differentially expressed genes encoding selected transcription factors, Toll-like and interleukin receptors are indicated.

